

Original Article

# To Study the Structural Characterization of the Polyaniline/CoFe<sub>2</sub>O<sub>4</sub> Nanocomposites

Seema<sup>1</sup>, Sunil Rohilla<sup>2</sup>, Sonia Arora<sup>3</sup>, Saneh Lata<sup>4</sup>, Anita Yadav<sup>5</sup>, Preeti kaushik<sup>6</sup>

<sup>1,3,4</sup> Department of Physics, M.N.S. Government College, Haryana, India.

<sup>2</sup> Department of Physics, Chaudhary Ranbir Singh University, Haryana, India.

<sup>6</sup> Department of Microbiology, CBLU, Haryana, India.

Received: 11 March 2022

Revised: 30 April 2022

Accepted: 05 May 2022

Published: 06 June 2022

**Abstract** - In the present research work, Polyaniline/CoFe<sub>2</sub>O<sub>4</sub> nanocomposites were prepared using the co-precipitation method, which is economical and eco-friendly. The CoFe<sub>2</sub>O<sub>4</sub> nanoparticles get adhered into a polymer using the in-situ chemical polymerization method. The various techniques were approached to characterize the prepared sample, such as XRD and FTIR. The peaks obtained at around 20.3 degrees and 25.2 degrees show the amorphous nature of PANI (low crystallinity). The appearance of characteristic diffraction peaks achieved at 35.5 degrees and 43.2 degrees ascribed to well-arranged crystalline cobalt ferrite pointing to the successive synthesis by co-precipitation route. Different analyses such as Debye-Scherrer, Halder, Wagner (H-W), and Williamson Hall (W-H) methods have investigated various parameters such as crystallite size and strain. The achieved values of crystallite size were highly correlated with Debye-Scherrer, Halder Wagner (H-W), and Williamson Hall (W-H) plots. The FTIR characterization confirmed the bonding among the Polyaniline/CoFe<sub>2</sub>O<sub>4</sub> nanocomposites, which gets well-matched with XRD results.

**Keywords** - Debye-Scherrer, Halder Wagner, PANI, Strain, W-H plots.

## 1. Introduction

Nanotechnology is the branch of study at the nanoscale; there are numerous classes of nanomaterials, such as polymeric nanomaterials are in great trend due to a wide range of applications. The polymeric nanocomposites possess a large conductivity, flexibility, and processability value. PANI (Polyaniline) is one of the most promising polymers attributed to its cost, easy synthesis, and chemical and thermal stability [1,14,26]. The magnetic and electrical properties of materials are important in sensors, absorbents, and shielding. The magnetic property of ferrite was enhanced by adhering to the conducting polymer [2,19]. Hence, the researchers focused on preparing polyaniline (PANI) and ferrite nanocomposites as they possess unique properties. The electronic and chemical interactions occur when the ferrite, a ferromagnetic material coated into a polymer matrix, is already conducting [16,17,18]. The ferrite particle gets incorporated into the polymer, improving and advancing the properties besides the conductivity in a controllable manner [3, 11]. Due to the high advancement in magnetic properties, ferrite is a promising material. Among ferrite, CoFe<sub>2</sub>O<sub>4</sub> is highly preferable due to its high coercivity value, anisotropy, the large value of magnetization, higher mechanical hardness, and stability [4,12]. The cobalt ferrite nanoparticles possess an inverse spinel structure to constitute ions of Fe<sup>3+</sup> and are distributed in an equal manner among the octahedral and tetrahedral sites. Therefore, in this article, we prepare and

characterize the PANI/CoFe<sub>2</sub>O<sub>4</sub> nanocomposites. The most important requisite factor among the nanostructured material is the size determination. X-ray diffraction tools can employ crystallite size and various phases. The obtained diffraction pattern for various phases is peculiar and termed fingerprint analysis of the prepared sample, which can be further matched with the JCPDS card of the various sample in the data Bank. In the investigation of the powdered sample through X-ray techniques, the data was obtained between the intensity and diffraction angle 2θ. In nanoscience, the Debye Scherrer formulation is considered the most extensively used to calculate the exact size of the prepared sample. Moreover, the broadening of peaks depends on various factors like strain, imperfection of lattice, and dislocation effects [5,13]. These defects should be minimized so that the width of the peak would be estimated more precisely. The strain present in the lattice structure that relies on ignition temperature is also responsible for broadening the peak [25]. A lot of structural investigations were done on the nanocomposites of polymer/ferrite. Debojyoti Nath et al. [6] studied the Williamson hall plots with different models under consideration for detecting microstructural and physical parameters like stress, energy density, and strain. The average granule size has been calculated from Debye Scherrer, Halder Wagner, and Williamson hall plots. M.A et al. [7] synthesized PANI/cobalt zinc ferrite having 5 M concentration nano substances by in-situ polymerization method. The nanocomposites were characterized by FTIR, X-ray diffraction, UV analysis, and TEM images. The



calculated average grain size of PANI (pure) and zinc Cobalt ferrite / PANI were 50 and 70 nanometers. In the present research work, the cobalt ferrite nanoparticles were prepared through the co-precipitation method, which is economical and eco-friendly. The  $\text{CoFe}_2\text{O}_4$  nanoparticles get adhered into a polymer using the in-situ chemical polymerization method. The structural characterization was done through XRD and FTIR investigation. Various analysis was employed, such as Debye Scherrer, Halder Wagner (H-W), and Williamson Hall plots (W-H). The obtained values of crystallite size and strain were in high correlation. The FTIR confirmed the bonding between PANI/ $\text{CoFe}_2\text{O}_4$ .

## 2. Starting Materials

The chemicals used in the present study are in the hydrated form of the salt of tin chloride, cobalt nitrate, ammonium hydroxide solution, and ethanol. The entire chemicals used in this research work are analytical grade and not to be further purified at a laboratory scale.

### 2.1. Synthesis

Pure PANI was prepared through the polymerization method. 0.4 M aniline gets dissolved into 50 ml HCl solution and sonicated it for almost  $\frac{1}{2}$  hr. 0.25 M ammonium persulfate gets mixed into the aniline + HCl solution and left the solution to polymerize under an ice bath approx. 24 hr. The greenish precipitates formed of PANI, filtered out, and dried out under vacuum conditions for one day. Cobalt ferrite nanoparticles were prepared through co-precipitation method [22,23,24]. Took the beaker and added a stoichiometric ratio of ferric chloride and cobalt chloride into a 50 ml water solution. Ammonium hydroxide pellets got mixed with 100 ml of water. They added the dropwise solution through the burette into the beaker with constant stirring on the hot plate at 70°C temperatures by maintaining a pH value between 8 to 9. The blackish powder was obtained as precipitates which were then filtered out and kept for the aging process for about 24 hrs. PANI/ $\text{CoFe}_2\text{O}_4$  nanocomposites were prepared through in situ chemical polymerization method by varying PANI composition with 0.2M and 0.3 M concentrations.

### 2.2. Properties examination of various samples

The characterization for the prepared nanostructured materials of PANI/ $\text{CoFe}_2\text{O}_4$  nanocomposites was conceded through diffraction caused by X-rays. The structural investigation of PANI/ $\text{CoFe}_2\text{O}_4$  nanocomposites nanostructured materials was examined using the XRD technique through Cu-K $\alpha$  radiation (0.154nm) by varying the angle position ranging from 10 to 80. Fourier Transform Infrared (FTIR) spectroscopy determined the infra-red spectrographs for the prepared PANI/ $\text{CoFe}_2\text{O}_4$  nanocomposites were determined through Fourier Transform Infrared (FTIR) spectroscopy. The X-rays and FTIR spectroscopic results were used to set up a relation between the crystalline nature of nanocomposites and strain values for the prepared PANI/  $\text{CoFe}_2\text{O}_4$  nanocomposites.

## 3. Results and Discussion

### 3.1. X-ray analysis

The graphical representation of PANI (pure) and PANI/ $\text{CoFe}_2\text{O}_4$  nanocomposites (with 0.2M and 0.3M heated at 300°C) are depicted in figure 1. The XRD diffraction peaks of cobalt ferrite get highly matched with the JCPDS card entry 22-1086, which constitute the cubic spinel structure of cobalt ferrite. The peaks obtained at around 20.3 degrees and 25.2 degrees show the amorphous nature of PANI (low crystallinity). The appearance of characteristic diffraction peaks achieved at 35.5 degrees and 43.2 degrees ascribed to well-arranged crystalline cobalt ferrite pointing to the successive synthesis by co-precipitation route. The weakening of diffraction peaks of PANI signified the incorporation of cobalt ferrite into polyaniline and confirmed the formation of nanocomposites. The grain size is calculated for the PANI/ $\text{CoFe}_2\text{O}_4$  nanocomposites (with 0.2M and 0.3M) at 21.33 nm and 14.28 nm, respectively, as obtained from the Debye Scherrer formulation.

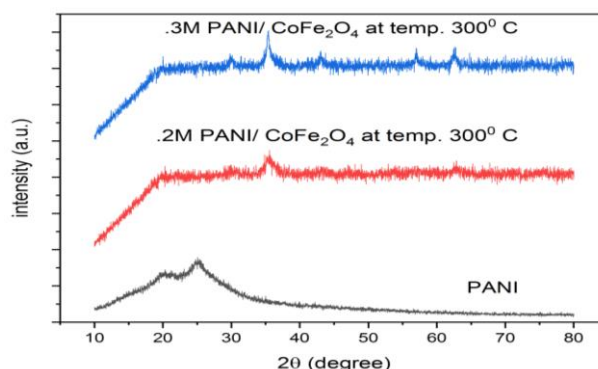


Fig. 1 Graphical representation of PANI/ $\text{CoFe}_2\text{O}_4$  nanocomposites (with pure PANI, 0.2M and 0.3M heated at 300°C)

### 3.2. Size determination

#### 3.2.1. Debye scherrer formula:

The crystalline size for the powdered sample for the intense peaks has been calculated through the Debye Scherrer formula:

$$D = \frac{K\lambda}{\beta \cos \theta}$$

Here, D represents the crystallite size in nm, K represents the Scherrer constant, and its value is .94,  $\lambda$  is the wavelength for Cu-  $k_{\alpha}$  radiation which constitutes the wavelength 0.154 nm,  $\theta$  is diffraction angle, and  $\beta$  is full width at half maximum intensity for the intense peak in radian unit. The average crystallite size and strain value for the PANI/ $\text{CoFe}_2\text{O}_4$  nanocomposites (0.2M) are 21.33 nm and  $0.10875 \times 10^{-3}$ , respectively. The average crystallite size and strain value for the PANI/ $\text{CoFe}_2\text{O}_4$  nanocomposites (0.3M) are 14.28 nm and  $0.1575 \times 10^{-3}$ , respectively.

### 3.2.2. Williamson hall plot (W-H plot):

With the addition of instrumental X-ray broadening, the pressure present within the lattice is also responsible for the peak broadening [8,15,20]. Hence the lattice stress highly affects the dimension of crystallite size. The whole peak broadening ( $\beta_T$ ) in the XRD pattern is the combination of broadening due to crystallite size ( $\beta$ ) and broadening due to stress ( $\beta_e$ ).

$$\beta_T = \frac{K\lambda}{\beta \cos \theta} + 4\epsilon \tan \theta$$

$\epsilon$  represents lattice strain in the crystal structure

$$\beta_T \cos \theta = \frac{K\lambda}{D} + 4\epsilon \sin \theta$$

The equation mentioned above represents a straight line; as a result,  $\epsilon$  is the line slope, and  $K\lambda/D$  is the intercept of a line. The Williamson hall plot for the PANI/CoFe<sub>2</sub>O<sub>4</sub> nanocomposites (0.2M and 0.3M) is plotted between the  $4 \sin \theta$  and  $\beta_T \cos \theta$ , as shown in figure 2. The crystallite size and lattice strain have been achieved from the intercept and slope of the linear fit of the curve. The size obtained for the (0.2M) PANI/CoFe<sub>2</sub>O<sub>4</sub> nanocomposites is 10.566 nm, and the achieved strain value is 0.00322. The achieved size for the (0.3M) PANI/CoFe<sub>2</sub>O<sub>4</sub> nanocomposites is 7.871 nm, and the strain value is  $4.95 \times 10^{-3}$ .

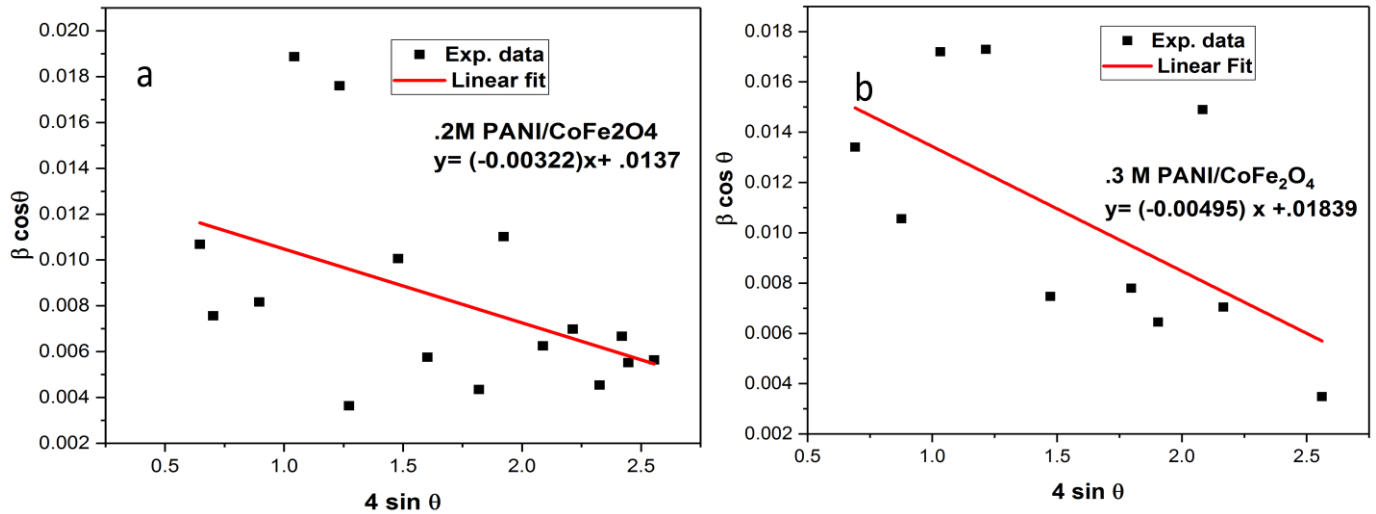


Fig. 2(a) W-H plot for the PANI/CoFe<sub>2</sub>O<sub>4</sub> nanocomposites (0.2M) (b) W-H plot for the PANI/CoFe<sub>2</sub>O<sub>4</sub> nanocomposites (0.3M)

### 3.2.3. Halder Wagner method (H-W plot):

This method is based on the supposition that broadening the peak is an asymmetric Voigt function as it combines both lorentzian and Gaussian functions. Hence, using the voigt function, the FWHM can be more accurately written through the Halder Wagner method as

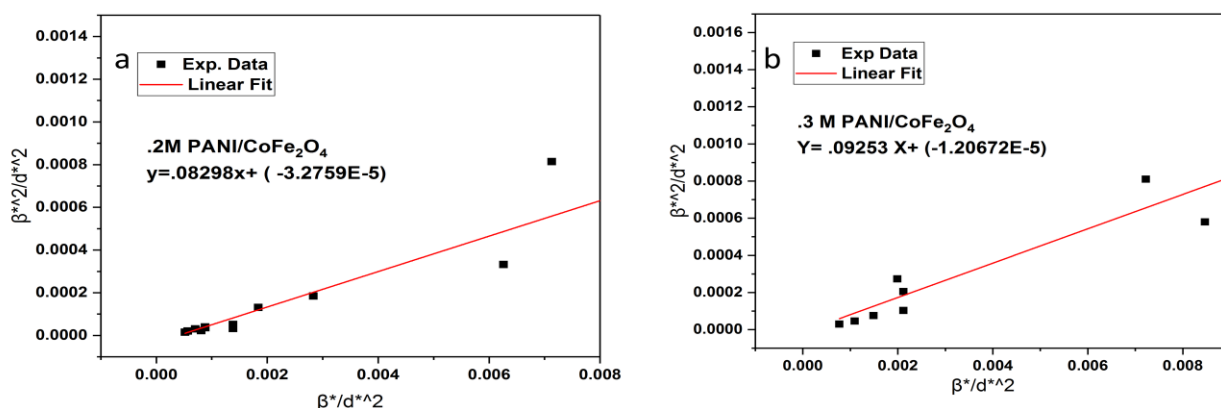
$$\beta_{hkl}^2 = \beta_L \beta_{hkl} + \beta_G^2$$

$\beta_L$  and  $\beta_G$  denote FWHM of laurentzian and gaussian function. This approach proves to be more advantageous as it focuses on the peak positions, which are situated to Lower-middle angle ranges where the overlapping of peaks is very less [9]. Hence the equation relates the crystallite size/lattice strain following the Halder Wagner technique is more precisely represented by:

$$\frac{\beta_{hkl}^{*2}}{d_{hkl}^{*2}} = \frac{1}{D} \cdot \frac{\beta_{hkl}^*}{d_{hkl}^{*2}} + \frac{\epsilon^2}{4}$$

Where  $\beta_{hkl}^* = (\beta \cos \theta)/\lambda$  and  $d_{hkl}^* = 2d \sin \theta / \lambda$

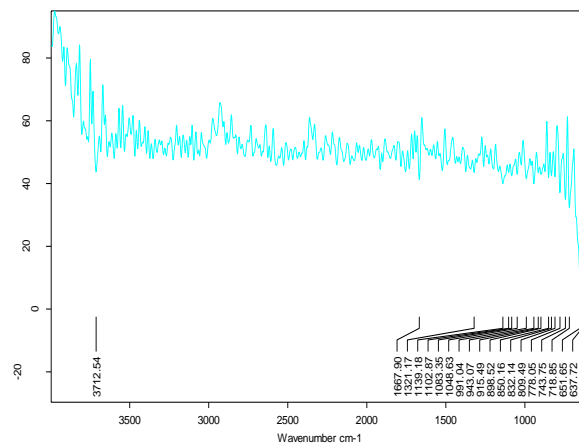
The graphical representation of the equation is shown in figure 3. The average crystallite size is obtained from the straight-line slope, and the lattice/intrinsic strain of the prepared sample is obtained by the intercept of the line. The mean crystallite size has been obtained from the graph for 0.2M PANI/CoFe<sub>2</sub>O<sub>4</sub> is 12.05 nm, and for 0.3M PANI/CoFe<sub>2</sub>O<sub>4</sub> is 10.80 nm which further suitably matched with the W-H plot. The estimated strain value by Halder Wagner comes out to be for sample 0.2M PANI/CoFe<sub>2</sub>O<sub>4</sub> is  $3.61 \times 10^{-5}$  and for sample 0.3M PANI/CoFe<sub>2</sub>O<sub>4</sub> is  $2.19 \times 10^{-5}$  which is obtained much more than the values achieved from another method. It is observed that the increment in the obtained strain values is basically due to the lower-middle angle XRD data. Moreover, the obtained values of strain in Halder Wagner, as shown in Table 1, because of the various dislocations present in the lattice site that plays a vital role in peak broadening at a much lower diffraction angle.

Fig. 3(a) H-W plot for the PANI (0.2M) /CoFe<sub>2</sub>O<sub>4</sub> nanocomposites (b) H-W plot for the PANI (0.3M) /CoFe<sub>2</sub>O<sub>4</sub> nanocompositesTable 1. Parameters for PANI/CoFe<sub>2</sub>O<sub>4</sub> nanocomposites

Sample	DebyeScherrer Method D(in nm)		Williamson-Hall method		Halder Wagner method	
	Size (nm)	strain	D (in nm)	Strain	D(in nm)	Strain
0.2M PANI/CoFe <sub>2</sub> O <sub>4</sub>	21.33	0.10875*10 <sup>-3</sup>	10.566	3.22*10 <sup>-3</sup>	12.05	3.61*10 <sup>-5</sup>
0.3M PANI/CoFe <sub>2</sub> O <sub>4</sub>	14.28	0.1575*10 <sup>-3</sup>	7.871	4.95*10 <sup>-3</sup>	10.80	2.19*10 <sup>-5</sup>

#### 4. FTIR

The FTIR spectroscopic examination of nano substances of PANI (0.2M and 0.3M) and Cobalt ferrite are displayed in figure 4 and Figure 5. The peak positions at 1510 cm<sup>-1</sup> and 1699 cm<sup>-1</sup> are ascribed to C=C stretched vibrations of benzenoid and quinoid rings. This validates the successful manufacturing of nanocomposites in the entire process. The broadband lying at position 1118 cm<sup>-1</sup> is mainly due to the C-N stretching vibrations [10]. These are the major characteristic peak position of FTIR spectra of PANI. The peak at 614 cm<sup>-1</sup> is ascribed to the account of various vibrations of the M-O cluster that arise from cobalt ferrite in the lattice site.

Fig. 4 FTIR spectrograph for PANI (0.2M)/CoFe<sub>2</sub>O<sub>4</sub> nanocomposites

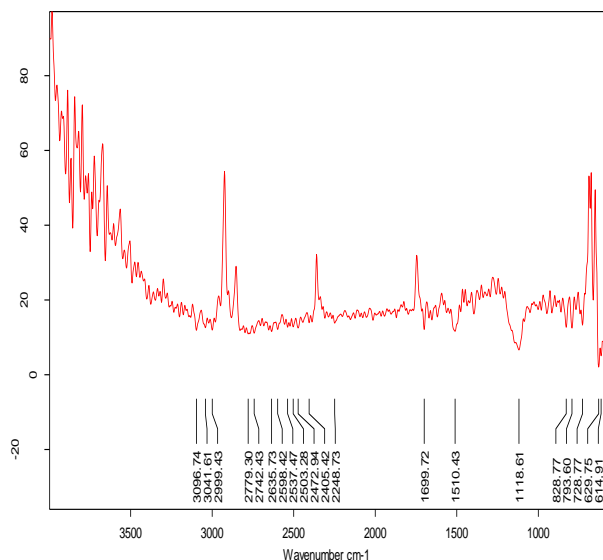


Fig. 5 FTIR spectrograph for PANI (0.3M)/CoFe<sub>2</sub>O<sub>4</sub> nanocomposites

## 5. Conclusion

In this research paper, the nanocomposites of PANI (0.2M)/CoFe<sub>2</sub>O<sub>4</sub> and PANI (0.2M)/CoFe<sub>2</sub>O<sub>4</sub> have been prepared, and various properties have been examined, which are summarized below:

1. The CoFe<sub>2</sub>O<sub>4</sub> nanoparticles were prepared through the co-precipitation route, which further gets adhered into the polymer (PANI) using the in-situ chemical polymerization method by varying the composition of PANI.
2. The structural characterization was done through XRD and FTIR investigation, which confirmed the formation of PANI/ CoFe<sub>2</sub>O<sub>4</sub>.
3. The average size and strain were analyzed using Debye Scherrer, Halder Wagner (H-W), and Williamson Hall plots (W-H).
4. The average sizes for the prepared nanocomposites were found to be decreased with an increase in PANI concentration due to atomic radii.

## Conflict of interest

The authors declare that there is no conflict of interest regarding the publication of this paper.

## References

- [1] M. Kooti, A. Naghdiseh, Kh. Gheisari, A. Figuerola. Synthesis, characterization, and performance of nanocomposites containing reduced graphene oxide, polyaniline, and cobalt ferrite, *Physica B: Condensed Matter* (612) (2021) 412974. DOI: <https://doi.org/10.1016/j.physb.2021.412974>
- [2] Tian Chen, Bo Liu. Dielectric properties of graphene quantum dot-cobalt ferrite-poly (vinylidene fluoride) ternary composites. *Materials Letters* 209 (2017) 163-166. DOI: <https://doi.org/10.1016/j.matlet.2017.07.088>
- [3] Ming Qin, Qin Shuaia, Guanglei Wu, Bohan Zheng, Zhengdong Wang, Hongjing Wub. Zinc ferrite composite material with controllable morphology and its Applications. *Materials science and engineering B* 224 (2017) 125-138. DOI: <https://doi.org/10.1016/j.mseb.2017.07.016>
- [4] Yuandong Penga, Yi Yi, Liya Li, Hengyu Ai, Xiaoxu Wang, Lulu Chen. Fe-based soft magnetic composites coated with NiZn ferrite are prepared by a co-precipitation method. *Journal of Magnetism and Magnetic Materials* 428 (2017) 148-153. DOI: <https://doi.org/10.1016/j.jmmm.2016.12.024>
- [5] Victor Y. Zenou, Snejana Bakardjieva. Microstructural analysis of undoped and moderately Sc-doped TiO<sub>2</sub> anatase nanoparticles using Scherrer equation and Debye function analysis. *Materials Characterization* 144 (2018) 287-296. DOI: <https://doi.org/10.1016/j.matchar.2018.07.022>
- [6] Debojyoti Nath, Fouran Singh, Ratan Das. X-ray diffraction analysis by Williamson- Hall, Halder-Wagner, and size-strain plot methods of CdSe nanoparticles-a comparative study. *Materials Chemistry and Physics* 239 (2020) 12-21. DOI: <https://doi.org/10.1016/j.matchemphys.2019.122021>
- [7] M.A. Gabal, A.A. Al-Juaid, S. El-Rashed, M.A. Hussein, Y.M. Al Angari. Polyaniline/Co<sub>0.6</sub>Zn<sub>0.4</sub>Fe<sub>2</sub>O<sub>4</sub> core-shell nanocomposites. Synthesis, characterization, and properties. *Journal of Alloys and Compounds* 747 (2018) 83-90. DOI: <https://doi.org/10.1016/j.materresbull.2010.06.021>
- [8] Rajesh Sharma, Anita Yadav, Sonia Arora, Nawal Kishore. To study the structural properties of cobalt doped tin oxide nanostructured by using Williamson-Hall and size-strain plot methodology. *Materials today: PROCEEDINGS* 44 (2021) 4651-4656 DOI: <https://doi.org/10.1016/j.matpr.2020.10.927>
- [9] Munmun Basak, Md. Lutfur Rahman, Md. Farid Ahmed, Bristy Biswas, Nahid Sharmin. X-ray diffraction peak profile analysis to determine the structural parameters of cobalt ferrite nanoparticles using Debye –Scherrer, Williamson- Hall, Halder – Wagner, and Size-Strain plot: Different precipitating agent approach. *Journal of Alloys and Compounds* 895 (2022) 162694. DOI: <https://doi.org/10.1016/j.jallcom.2021.162694>
- [10] Hongbo Gu, Hongyuan Zhang, Jing Lin, Qian Shao, David P. Young, Luyi Sun, T.D. Shen, Zhanhu Guo, Large negative giant magnetoresistance at room temperature and electrical transport in cobalt ferrite-polyaniline nanocomposites. *Polymer* 143 (2018) 324-330.
- [11] kasala suresha, thermoelectric power in wide bandgap semiconductor ZnO nanowire, *SSRG International Journal of Applied Physics*, 9(1) (2022) 9-11. <https://doi.org/10.14445/23500301/IJAP-V9I1P102>
- [12] Firoz Ahmed, Md. Ibrahim, H. Mondal, Md. Nazmul Huda, Md. Khademul Islam, Nano ZnO Loaded Trimethyl Chitosan Chloride- A



- promising Bio-composite for Antimicrobial and wound Healing Fabric. SSRG International Journal of Applied Physics, 9(1) (2022) 6-10 <https://doi.org/10.14445/23942592/IJPTE-V9I1P102>
- [13] K. vimala, Y.M. Mohan, K. Varaprasad, N.N. Redd, S. Ravindra, NS. Naidu, Fabrication of curcumin Encapsulated Chitosan PVA Silver nanocomposite films for improved Antimicrobial activity, Journal of Biomaterials and Nanobiotechnology. 2(2011) 55-64.
- [14] R.Laur, D.Goyal, S.Agnihotri, Chitosan/PVA silver nanocomposite for Butachlor Removal: Fabrication, characterization, adsorption Mechanism and isotherms, carbohydrate polymers. 262 (2021) 117906.
- [15] M.K. Hassan, A. Abukmail, A.J. Hassiba, K.A. Mauritz, A. Elzatahry, PVA/Chitosan/Silver nanoparticles electrospun nanocomposites: Molecular relaxations investigated by modern broadband Dielectric Spectroscopy, Nanomaterials. 8(11)(2018) 888.
- [16] R.Rajendran, C. Balakumar, H.A.M. Ahamed, S. Jayakumar, k. Vaideki, E.M. Rajesh, Use of zinc oxide nanoparticles for production of antimicrobial textiles, International Journal of Engineering, Science and Technology. 2(1) (2010) 202-208.
- [17] B. jeevanantham, Youngseoksong, Heemanchoe, M.K. Shobana, Structural and optical characteristics of cobalt ferrite nanoparticles, Materials Letters: X 12(2021) 100-105, <https://doi.org/10.1016/j.mblux.2021.100105>
- [18] Deepali, D. Andhare, Supriya, R. patade, Jitendra S. Kounsalye, K.M. Jadhav. Effect of Zn doping on structural, magnetic, and optical properties of cobalt ferrite nanoparticles synthesized via. Co-precipitation method. Physica B: Condensed Matter 583(2020) 412051. <https://doi.org/10.1016/j.physb.2020.412051>
- [19] Bikramjit Kaur, Ruchika Tanwar, Uttam K. Mandal. Effect of calcination and surface Functionalization of nanoparticles on structural, magnetic, and electrical properties of polyaniline Ni<sub>5</sub>Zn<sub>5</sub>Fe<sub>2</sub>O<sub>4</sub> nanocomposites. Colloids and surfaces A: physicochemical and Engineering Aspects. 628 (2021) 127273. <https://doi.org/10.1016/j.colsurfa.2021.127273>
- [20] M. M. Bagheri, M. Valid, A. Gholipour, P. Makvandi, E. Sharifi, Chitosan Nanofiber Biocomposites for Potential Wound Healing Applications: Antioxidant Activity with Synergic Anti-Bacterial Anti-Bacterial Effect, Bioengineering & Translational Medicine. 7(1) (2022) 10254
- [21] P.S.V. Shanmukhi, Dr. K. Chandramouli and Dr. P.V.S. Machiraju, (2016) Investigative Study of Structural morphology of Polypropylene and BaCo<sub>3</sub> – Nanoparticle Composites. SSRG International Journal of Material Science and Engineering 2(3), 8-12.
- [22] Seema Sharma, Sunil Rohilla, Synthesis of nanocomposites of NiFe<sub>2</sub>O<sub>4</sub>/SiO<sub>2</sub> through co-precipitation method and structural characterization using Rietveld refinement, AIP Conference Proceedings 2270, (2020) 110023 <https://doi.org/10.1063/5.0020045>.
- [23] Haibo Yang, Ting Ye, Ying Lin, Jianfeng Zhu, Fen Wang, Microwave absorbing properties of the ferrite composites based on graphene. Journal of Alloys and Compounds 683 (2016) 567-574.
- [24] Moonis Ali Khan, Mohammad Mezbaul Alam, Mu Naushad, Zeid Abdullah Alotman, Mahendra Kumar, Tansir Ahamad Sol-gel assisted synthesis of porous nano-crystalline CoFe<sub>2</sub>O<sub>4</sub> composite and its application in the removal of brilliant blue-R from aqueous phase: An eco-friendly and economical approach. Chemical Engineering Journal 279 (2015) 416–424.
- [25] Duan Wang, Jingli Wu, Daxun Bai, Rongrong Wang, Feng Yao, Sailong Xu, Mesoporous spinel ferrite composite derived from a ternary MgZnFe-layered double hydroxide precursor for lithium storage. Journal of Alloys and Compounds 726 (2017) 306-314. DOI: <https://doi.org/10.1016/j.polymer.2018.04.008>
- [26] R. Nawalakhe, Q. Shi, N. Vitchuli, J. Noar, J.M. Caldwell, F. Breidt, M.A. Bourham, X. Zhang, M.G. McCord, Novel Atmospheric Plasma Enhanced Chitosan Nanofiber/Gauze Composite Wound Dressings, Journal of Applied Polymer Science. 129(2) (2013) 916- 923.